Cancer Immunology, Immunotherapy (2019) 68:1121–1132
https://doi.org/10.1007/s00262-019-02345-5

ORIGINAL ARTICLE

Patterns of immune-cell infiltration in murine models of melanoma: roles of antigen and tissue site in creating inflamed tumors

Katie M. Leick[1,2,4] · Joel Pinczewski[1,3] · Ileana S. Mauldin[1,4] · Samuel J. Young[4,7] · Donna H. Deacon[1,4] · Amber N. Woods[4,5] · Marcus W. Bosenberg[6] · Victor H. Engelhard[4,5] · Craig L. Slingluff Jr.[1,4]

Received: 13 June 2018 / Accepted: 8 May 2019 / Published online: 27 May 2019

Abstract

Immune-cell infiltration is associated with improved survival in melanoma. Human melanoma metastases may be grouped into immunotypes representing patterns of immune-cell infiltration: A (sparse), B (perivascular cuffing), and C (diffuse). Immunotypes have not been defined for murine melanomas, but may provide opportunities to understand mechanism-driving immunotype differences. We performed immunohistochemistry with immune-cell enumeration, immunotyping, and vascular density scoring in genetically engineered (Braf/Pten and Braf/Pten/β-catenin) and transplantable (B16-F1, B16-OVA, and B16-AAD) murine melanomas. The transplantable tumors were grown in subcutaneous (s.c.) or intraperitoneal (i.p.) locations. Braf/Pten and Braf/Pten/β-catenin tumors had low immune-cell densities, defining them as Immunotype A, as did B16-F1 tumors. B16-OVA (s.c. and i.p.) and B16-AAD s.c. tumors were Immunotype B, while B16-AAD i.p. tumors were primarily Immunotype C. Interestingly, the i.p. location was characterized by higher immune-cell counts in B16-OVA tumors, with counts that trended higher for B16-F1 and B16-AAD. The i.p. location was also characterized by higher vascularity in B16-F1 and B16-AAD tumors. These findings demonstrate that spontaneously mutated neoantigens in B16 melanomas were insufficient to induce robust intratumoral immune-cell infiltrates, but instead were Immunotype A tumors. The addition of model neoantigens (OVA or AAD) to B16 enhanced infiltration, but this most often resulted in Immunotype B. We find that tumor location may be an important element in enabling Immunotype C tumors. In aggregate, these data suggest important roles both for the antigen type and for the tumor location in defining immunotypes.

Keywords B16 melanoma · Immunotype · Vascular density · Immune-cell density

Abbreviations

AR	Antigen retrieval buffer
DAB	3,30-Diaminobenzidine
Hpf	High-power field
TLS	Tertiary lymphoid structure

Précis High mutational load alone is insufficient to drive high immune-cell density and diffuse T-cell distribution in murine melanomas; however, strong antigen can induce a robust immune response, which is enhanced by intraperitoneal tumor location.

✉ Craig L. Slingluff Jr.
cls8h@virginia.edu

[1] Division of Surgical Oncology, Department of Surgery, University of Virginia, P. O. Box 800709, Charlottesville, VA 22908-0709, USA

[2] Department of Surgery, University of Iowa, Iowa City, IA, USA

[3] Department of Pathology, Dorevitch Pathology, Melbourne, Australia

[4] Beirne Carter Center for Immunology Research, University of Virginia, Charlottesville, VA, USA

[5] Department of Microbiology, Immunology, and Cancer Biology, University of Virginia, Charlottesville, VA, USA

[6] Departments of Dermatology and Pathology, Yale University, New Haven, CT, USA

[7] University of Virginia Cancer Center, Charlottesville, VA, USA

Introduction

Immune-cell infiltration into the tumor microenvironment is associated with improved survival and clinical response to immune therapies in melanoma; thus, a goal of combination immunotherapy is to enhance immune-cell infiltration [1–8]. We previously showed that infiltration into human melanoma metastases can be categorized into three distinct immunotypes that are associated with patient survival. Immunotype

A is sparsely infiltrated with immune cells, Immunotype B is characterized by immune-cell cuffing around intratumoral vessels, and Immunotype C is characterized by diffuse intratumoral immune-cell infiltrates [1]. Murine models facilitate preclinical studies leading to mechanistic understanding of factors that underlie each immunotype, yet murine models of each immunotype have not been defined. Thus, it is useful to identify murine models that reflect each of the immunotypes of human melanoma and to understand how features of those models influence the patterns and extent of immune infiltration.

Established murine models for melanoma include both genetically engineered and spontaneous tumors. Braf/Pten and Braf/Pten/β-catenin (mutated Braf, Pten knockout, and stabilization of β-catenin [9]) mice are genetically engineered to enable the induction and outgrowth of melanomas under the influence of genetic alterations that reflect the molecular and oncogenic signature pathways that drive tumor formation in human melanoma [9, 10]. However, they have a low density of immune infiltrates [11–13], thought to reflect their low mutational burden and consequent lower immunogenicity [14, 15]. Patterns of immune-cell distribution in the Braf/Pten models have not been previously described. We hypothesized that, despite the presence of genetic driver mutations of melanoma in the Braf/Pten models, their low number of spontaneous mutations will result in sparse immune-cell infiltration (Immunotype A). On the other hand, the transplantable B16 murine melanoma cell line has a high mutational burden comparable to that seen in human melanomas [14–16], though the oncogenic drivers underlying its formation have not been established. One might expect that those mutations would support immune-cell infiltrates, but the previous work from our group has demonstrated a low density of immune infiltrates in B16-F1 melanoma [11]. Immune-cell infiltrates are enhanced when B16-F1 cells are transfected with ovalbumin (B16-OVA) [11]. However, the spatial distribution of immune cells in B16-OVA tumors has not been defined. In addition, differences in homing receptor ligands in s.c. compared to i.p. compartments directly impact immune infiltration and lead to increased infiltration in peritoneal tumor implants [17]. However, the impact of tumor site on immune infiltration is not well-studied. We hypothesized that B16 melanomas transfected with xenogeneic antigens would induce immune-cell infiltrates consistent with either Immunotypes B and C and that the immunotypes may be impacted by the nature of the antigen and the tissue site.

The goals of the present study were to define patterns of immune-cell infiltrates in Braf/Pten and B16 murine models and to determine whether these are similar to immunotypes observed in human melanoma metastases, and also to provide mechanistic insights into factors that influence immunotypes in these murine models. We included B16 melanomas transfected to express either the model antigen ovalbumin (B16-OVA) or the chimeric class I MHC molecule AAD (B16-AAD) to test whether addition of a strong "neoantigen" enhances immune infiltration and thereby alters the immunotype. We test whether immunotype is intrinsic to the malignant cell type or whether it may be modulated by the site of tumor outgrowth, as this may have implications for intra-patient heterogeneity in humans. Since immune-cell infiltration also depends on extravasation from tumor vasculature [17, 18], we also assessed tumor vascularity among different melanomas in two anatomical sites. These studies contribute to understanding the role of antigen and tumor site in defining immunotype and density of immune infiltrates in murine tumors.

Materials and methods

Cell lines

B16-F1 parental cell lines were transfected with OVA [19] and AAD [20] constructs as previously described. AAD is a chimeric class I MHC molecule comprised of the $\alpha1+\alpha2$ domains of human HLA-A*0201 and the $\alpha3$ domain of murine H-2D^{d} [21]. Transfectants were cultured in RPMI-1640 containing 5% FBS supplemented with SerXtend (Irvine Scientific, Santa Ana, CA) and 300 µg/ml G418 (Life Technologies, Grand Island, NY), and screened regularly by flow cytometric analysis for AAD expression using the HLA-A2-binding antibodies CR11-351 or BB7.2. To establish tumors, 4×10^{5} tumor cells were injected s.c. in the nape of the neck, or i.p., to establish solid tumors in the subcutaneous space or i.p. cavity, respectively. Tumors were allowed to establish 10–14 days for i.p. and s.c. before harvest.

Animals

C57BL/6 mice (NCI-Frederick Animal Production Program) were maintained in pathogen-free facilities at the University of Virginia. Protocols were approved by the University of Virginia Institutional Animal Care and Use Committee.

Braf/Pten tumors

Tumors were induced in 3-week-old *Tyr-CreER/Pten^{lox}/Braf^{CA}* and *Tyr-CreER/Pten^{lox}/Braf^{CA}/Ctnnb1^{loxex3}* transgenic mice using methods previously described [9, 10], and harvested when they reached 1 cm^{3} in volume (approximately 6–8 weeks later). Formalin-fixed paraffin-embedded blocks were prepared from these tumors.

Human tumors

Immunohistochemistry was performed on human melanomas on tissue microarrays, which were prepared as previously described [1].

Immunohistochemistry and tumor cross-sectional area measurements

Tissue sections from human and murine tumors were deparaffinized and hydrated with xylene and graded alcohol series. Antigen retrieval wasperformed with target retrieval solution (Dako North America, S2367), pH 9, at 100 °C for 20 min. Sections were stained with a triple combination of antibodies specific for S100 (Human and Mouse: Cat# Z0311, Dako North America, Carpinteria, CA), CD45 (Human: Clone # PD7/26/16 + 2B11, Dako North America; Mouse: Clone # 30-F11, BD Biosciences San Jose, CA), and CD31 (Human: Clone # JC70A, Dako North America; Mouse: Clone # SZ31, Dianova GmbH, Hamburg, Germany). Detection was made using ImmPRESS HRP kits Anti-rabbit Ig MP-7401, Anti-mouse Ig MP-7402, and Anti-rat Ig MP-7044, and ImmPACT HRP Substrates 3,30-diaminobenzidine (DAB), SG Peroxidase (Blue/Gray), and VIP Peroxidase (Purple) (all from Vector). Sections were cover-slipped with mounting medium (Vector) after they were rinsed with water. Negative control slides were prepared by omitting the primary antibodies. ImageJ was used to manually draw a region of interest around each tumor, and tumor cross-sectional area was calculated in mm^2 using the measure function in ImageJ and was converted to high-power fields (hpfs).

Quantification of TIL, immunotyping, and vascularity scoring

Enumeration of $CD45^+$ cells was performed by a trained pathologist (J Pinczewski) on representative sections triple stained with S100, CD45, and CD31 in 10 independent hpfs for each tumor. Cells within blood vessels or necrotic tumor areas were excluded. Immunotype was assigned (J Pinczewski) using criteria previously defined in our laboratory [1]. If there were less than 15 $CD45^+$ cells per hpf (~ 50 per mm^2) based on the average of 10 hpfs, the tumor was classified as Immunotype A, regardless of distribution. A $CD45^+$ cell density of 15 per hpf or greater was classified as Immunotype B or C, depending on cell distribution. The entire tumor section was evaluated for overall pattern of distribution. Immunotype B was classified by a predominant perivascular distribution of $CD45^+$ cells, and Immunotype C was classified by a predominant diffuse intratumoral immune infiltration irrespective of perivascular cuffing. Vascularity scoring was performed by a certified pathologist (J Pinczewski) who was blinded to the origin of the samples based upon $CD31^+$ staining vessels. A scant number of vessels were represented by a score of 1, a moderate number of vessels by a score of 2, and a large number of vessels by a score of 3. Images were obtained using an Olympus (Center Valley, PA) BX51 microscope coupled to an Olympus BP70 digital camera and analyzed using Image ProPlus 4.5 for the Windows software.

Multispectral Imaging and immune-cell subset enumeration

4-µm-thick sections were cut from formalin-fixed paraffin-embedded murine tumor specimens, and murine spleen was used as a positive control. Multispectral staining was performed according to the manufacturer's protocol using the OPAL Multiplex Manual IHC kit and antigen retrieval buffer (AR) 9 (PerkinElmer, Waltham, Massachusetts, USA). Staining sequence, antibodies, and antigen retrieval buffers were as follows: AR9, CD4 (dilution 1:100; Abcam, Cambridge, Massachusetts, cat#ab183685) Opal520; AR9, CD8 (1:200, Abcam, cat#ab237723) Opal540; AR9, CD34 (1:400, Abcam, cat#81289) Opal620; AR9, CD19 (1:50; Cell-Signaling Technology, Danvers, Massachusetts, cat#90176S); and spectral DAPI (PerkinElmer, Waltham, Massachusetts, USA). Slides were mounted using prolong diamond antifade (Life Technologies, Carlsbad, California, USA) and scanned at 10× magnification using the PerkinElmer Vectra 3.0 system and Vectra software (PerkinElmer, Waltham, Massachusetts, USA). Regions of interest were then identified in the Phenochart software, and 20× magnification images were acquired with the Vectra 3.0 system. These images were spectrally unmixed using single-stain positive controls and analyzed using the InForm software (PerkinElmer, Waltham, Massachusetts, USA). Enumeration of immune-cell subsets was performed using an algorithm generated with the InForm software and validated manually (KM Leick).

Statistical analysis

Analyses were performed with the GraphPad Prism 7 software. Student's *t* test was used to compare two groups. One-way ANOVA with Tukey's post-test was used to compare more than two groups and two-way ANOVA with Bonferroni correction was used to compare data grouped by two variables. A *P* value of less than 0.05 was considered to be significant.

Results

In prior work, we assessed the localization and density of $CD45^+$ immune cells relative to intratumoral vasculature in human melanoma metastases to define Immunotypes using

single-stain IHC in three consecutively cut sections. To improve our assessments, we developed an approach to triple-stain single sections of human and murine tumors using antibodies to CD45 (immune cells), CD31 (vasculature), and S100 (melanoma cells). Examples of this approach applied to human melanoma metastases are shown in Fig. 1. This serves as a better method for immunotyping by allowing the pathologist to more reliably distinguish cellular spatial relationships within a single-tissue section instead of making comparisons across several individually stained tissue sections.

We used this approach to analyze 9–11-week-old dermal melanomas induced at 3 weeks of age in Braf/Pten and Braf/Pten/β-catenin transgenic mice ($n=3$ each). For all six tumors, there were only rare immune cells (< 15/hpf, Fig. 2). Others have shown that the activation of the β-catenin pathway is associated with immune-cell exclusion from tumors [22]. However, there was no significant difference in immune infiltration between Braf/Pten and Braf/Pten/β-catenin given the number of evaluable tumors. The $CD45^+$ cell counts for Braf/Pten tumors ranged from 0.2 to 8.9 per hpf and from 0 to 2.7 per hpf for Braf/Pten/β-catenin tumors (Fig. 2c). Thus, we classified those tumors as Immunotype A.

On the other hand, in B16 models, we found examples of Immunotypes A (Fig. 3a, d), B (Fig. 3b, e), and C (Fig. 3c, f) that were strikingly similar to the immunotypes defined in human melanoma. We then asked whether the more densely infiltrated Immunotype C and B tumors have decreased tumor outgrowth compared to the more sparsely infiltrated Immunotype A tumors, similar to that shown in humans [1]. Measurement of tumor cross-sectional areas demonstrated significantly reduced tumor burden in Immunotype B and C tumors compared to Immunotype A tumors (Fig. 4a). This suggests that immunotypes in murine tumors have functional implications in tumor outgrowth that are reflected in human melanomas.

We then assessed B16 melanoma models based on tumor type and tissue site. Despite the expression of a large number of mutated neoantigens in parental B16-F1 melanomas [16], 11 of 12 B16-F1 tumors were exclusively Immunotype A, independent of tumor location (Fig. 4b). Mean $CD45^+$ counts for B16-F1 were 0.1 ± 0.1 (SD) and 7.6 ± 12 cells/hpf for s.c. and i.p tumors, respectively, without significant differences between tumor sites (Fig. 4b). B16-OVA tumors express one strong neoantigen for T cells, presented by H-2 K^b, and are more extensively infiltrated by T cells compared to B16-F1 [11]. In keeping with this, and in contrast to B16-F1, 9/10 B16-OVA tumors were Immunotype B, independent of tumor location (Fig. 4b). Interestingly, however, the $CD45^+$ counts in B16-OVA tumors were significantly and dramatically higher in i.p. sites (321 ± 206 cells/hpf) than in s.c. sites (27 ± 15 cells/hpf, $P < 0.0001$, Fig. 4b). B16-AAD tumors are generated through transfection of a gene encoding the human/murine chimeric HLA molecule AAD, resulting in expression of a xenogeneic MHC-I molecule that can present multiple endogenous peptides [21] and may also serve as a xenoantigen for antibody recognition; however, the influence of this antigen on immune infiltration is not known. As with B16-OVA, s.c. B16-AAD tumors were also predominantly (4/5) Immunotype B. In contrast, most (3/5) i.p. B16-AAD tumors were Immunotype C (Fig. 4b). In B16-AAD, the $CD45^+$ counts trended higher in i.p tumors (77 ± 50 cells/hpf, Fig. 4b) compared to s.c. tumors (19 ± 7 cells/hpf, Fig. 4b). Thus, introduction of either strong antigen (OVA or AAD) in B16 melanoma results in a greater density of immune cells compared to

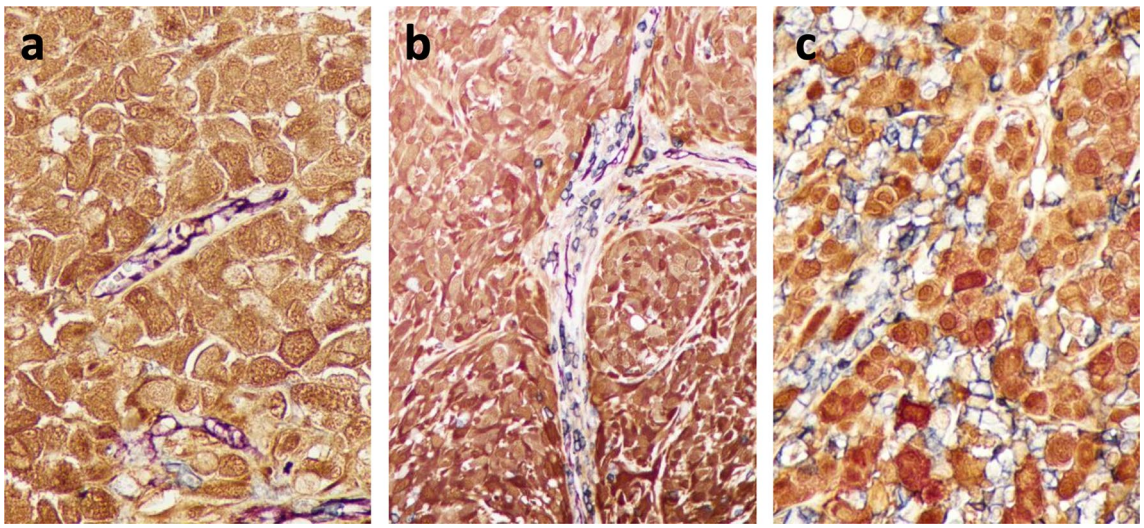

Fig. 1 Immunotype A, B, and C human melanoma metastases, respectively. Tissue sections were triple stained with antibodies to CD31 (vascular endothelium, purple), CD45 (immune cells, blue), and S100 (melanoma cells, brown)

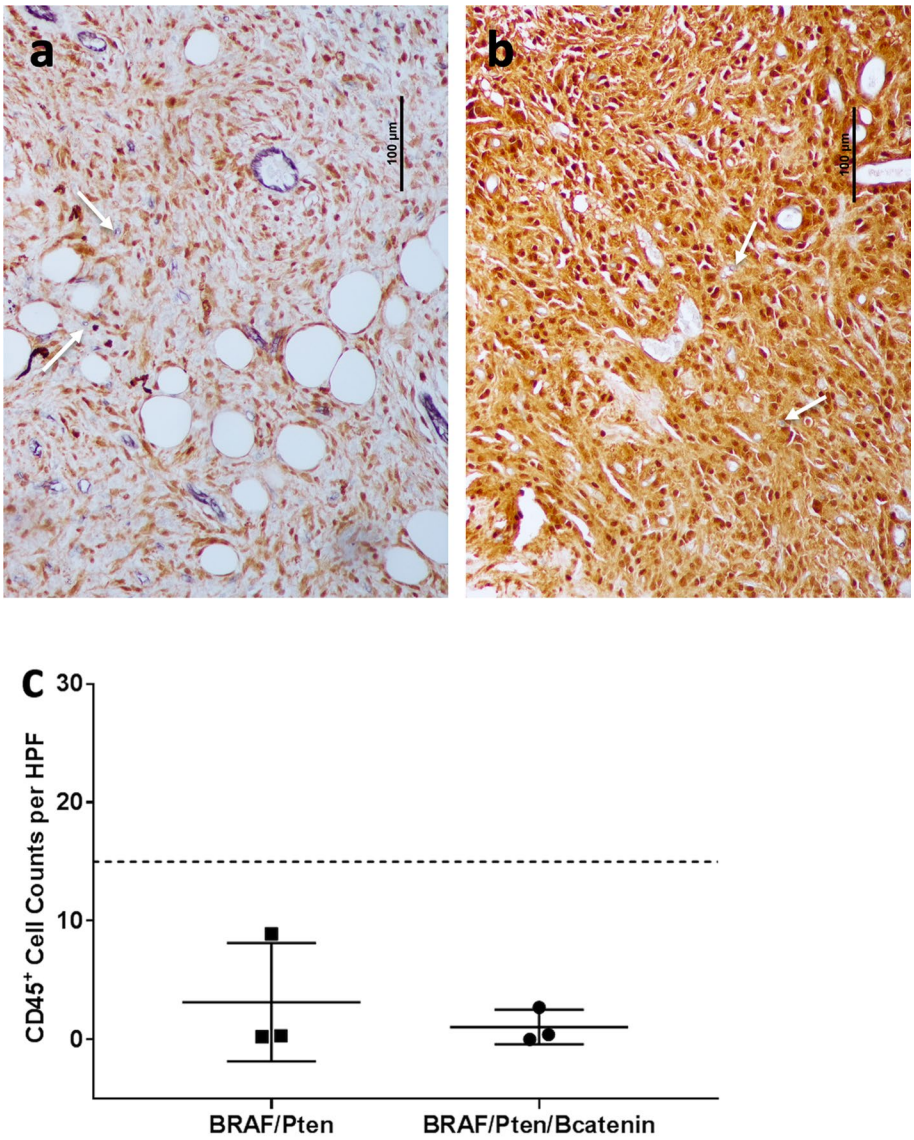

Fig. 2 Immunotype and immune-cell density of spontaneous murine melanomas. Representative examples of Braf/Pten (**a**) and Braf/Pten/β-catenin (**b**) dermal melanomas were triple stained with antibodies to CD31 (vascular endothelium, purple), CD45 (immune cells, blue), and S100 (melanoma cells, brown). Quantification of CD45 counts per 10 hpf of Braf/Pten ($n=3$) and Braf/Pten/β-catenin ($n=3$) murine melanoma (**c**) with dashed line at 15 to indicate cutoff for Immunotype A and white arrows to indicate $CD45^+$ immune cells

parental B16-F1. While expression of either strong antigen induced Immunotype B tumors in s.c. locations, AAD expression was unique in inducing Immunotype C tumors selectively in i.p. locations.

In patients with melanoma, Immunotype C tumors have higher immune-cell density than Immunotype B [1]. Therefore, we hypothesized that Immunotype C murine tumors would be more robustly infiltrated than Immunotype B tumors. The $CD45^+$ counts for Immunotype B and C tumors were higher than for Immunotype A tumors ($P=0.006$ and $P=0.052$, respectively; Fig. 4c). Interestingly, there was wide variation among those counts in Immunotype B tumors. Thus, we assessed whether cell count variation could be explained by antigen (OVA vs AAD) and/or tumor site. Among B16-AAD tumors, $CD45^+$ cell density did not differ between s.c. and i.p. sites. However, in B16-OVA tumors, $CD45^+$ density was greater in the i.p. site, with wide variation among these counts (Fig. 4b, c). $CD45^+$ densities for B16-OVA i.p. were higher than B16-AAD i.p. ($P=0.009$, Fig. 4b), despite the fact that the pattern of infiltrate was more diffuse (mostly Immunotype C) for B16-AAD i.p. (Figure 4b). This suggests that the pattern of infiltrate is not simply a surrogate for immune-cell density and that both tumor location and the nature of the tumor antigens may independently impact immune-cell density and immunotype.

To determine whether there was a predominance of a particular immune-cell subset related to immunotype, tumor type, or location, we evaluated the B16 tumors with multiparameter immunofluorescence staining for $CD8^+$ and $CD4^+$ T cells, $CD19^+$ B cells, and $CD34^+$ vasculature, with examples of Immunotypes A (Fig. 5a), B (Fig. 5b, d, e), and C (Fig. 5e). Immunotype C and Immunotype B tumors

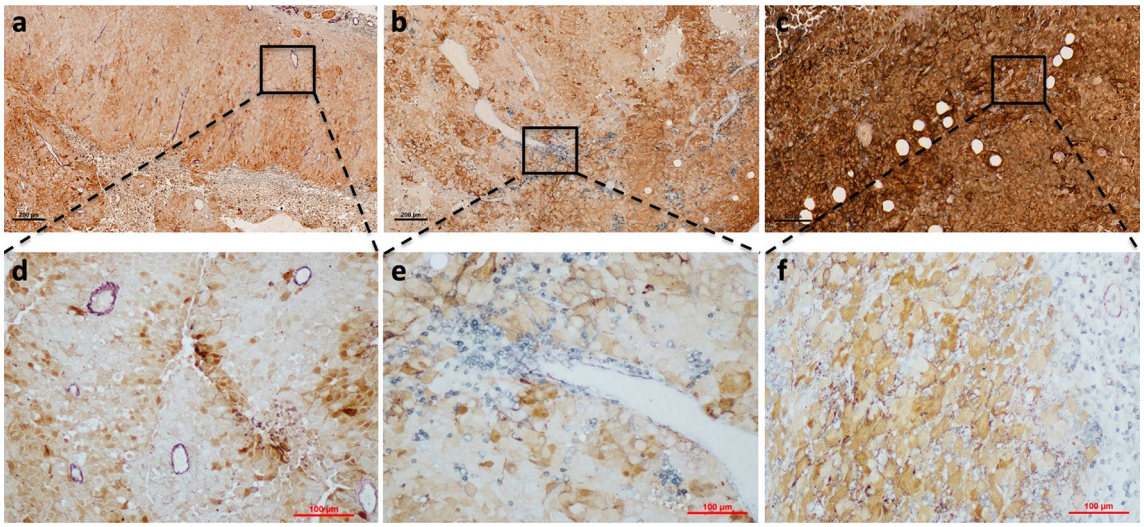

Fig. 3 Representative images of B16 tumors demonstrate Immunotypes A, B, and C. All tumors were triple stained with antibodies to CD31, CD45, and S100. A representative image of a s.c. B16-F1 tumor classified as Immunotype A with low- (**a**) and high (**d**)-power views. (**b**) Low-power and high-power (**e**) views of a s.c. B16-AAD tumor categorized as Immunotype B. (**c**) A low and high (**f**) power view of i.p. B16-AAD tumor of melanoma classified as Immunotype C

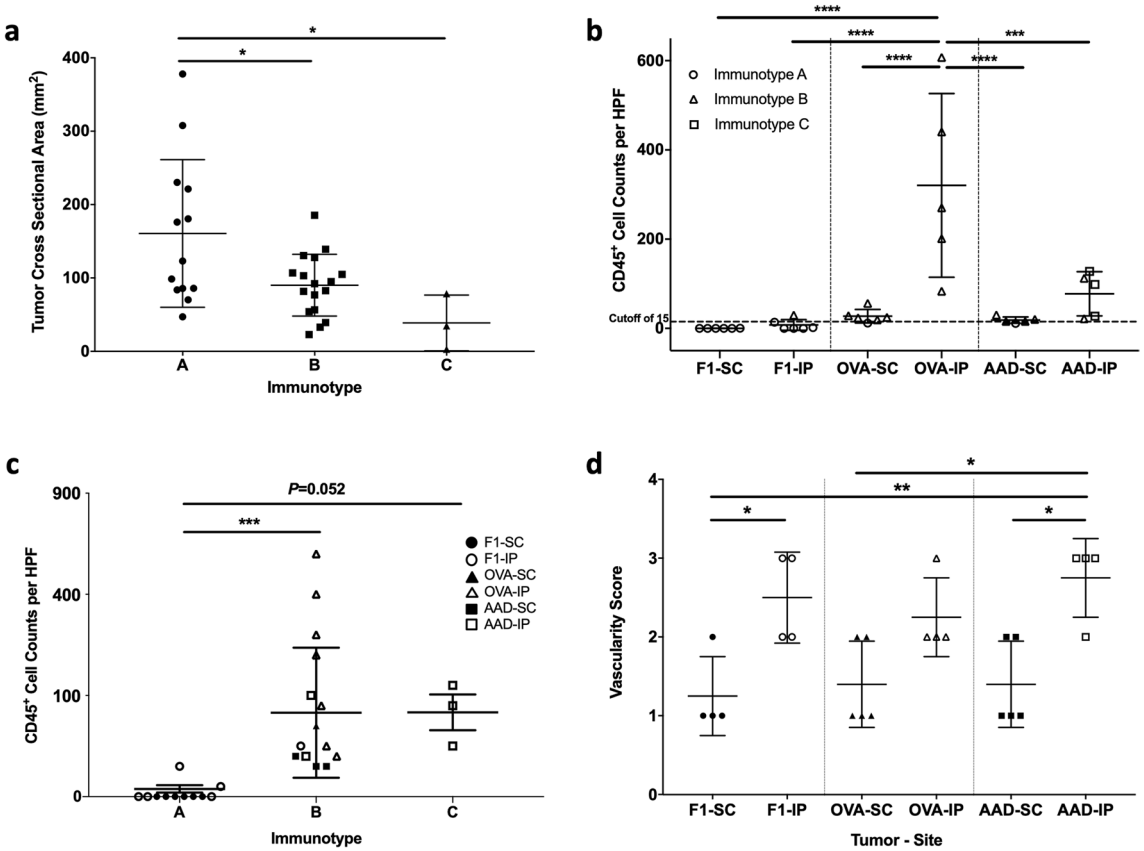

Fig. 4 Associations of B16 tumor cell type and tumor location with tumor cross-sectional area, immune infiltrate, and vascularity. B16-F1 melanomas, or those transfected with OVA or AAD, were grown in s.c. or i.p. locations and evaluated for tumor cross-sectional area in mm^2 using ImageJ (a) and overall $CD45^+$ cell counts with dashed line at 15 to indicate cutoff for Immunotype A (b) and vascularity (d). (c) $CD45^+$ cell counts were quantified across 10 *high-powered fields* in Immunotype A ($n=13$), Immunotype B ($n=17$), and Immunotype C ($n=3$). This included s.c. and i.p. tumors from each B16 model. Differences were assessed by one-way ANOVA, with significance noted by asterisks: * < 0.05, ** < 0.01, *** < 0.001, **** < 0.0001

were more robustly infiltrated with $CD8^+$ and $CD4^+$ T cells than Immunotype A tumors (Fig. 5f), while there was a trend towards higher B-cell counts in Immunotypes B and C ($P = 0.1$, Fig. 5f). This is consistent with higher overall $CD45^+$ cell counts in Immunotypes B and C in these tumors (Fig. 4c). Characterization of the immune-cell subsets based on tumor type and location demonstrated significantly higher density of $CD8^+$ T cells in B16-AAD i.p. tumors than B16-OVA and B16-F1 tumors, but not significantly higher than B16-AAD s.c. tumors (Fig. 6a). This suggests that the AAD antigen may induce a strong $CD8^+$ T-cell response. B16-AAD i.p. tumors also had significantly higher densities of $CD4^+$ T cells than all other tumors except for B16-OVA i.p (Fig. 6b), indicating an important role for $CD4^+$ T cells in both B16-OVA and B16-AAD, and specifically in the i.p. location. Interestingly, the highest B-cell densities were in B16-OVA i.p. and B16-AAD i.p. tumors (Fig. 6c). B16-F1 and OVA s.c. tumors had low numbers of immune-cell subsets overall. We also considered the lymphocyte subset composition in terms of percentages, finding that proportions of $CD8^+$ T cells trended higher in s.c. sites, whereas B cells trended higher in i.p. sites among all three B16 tumors (Fig. 6d, f). $CD4^+$ T cells proportionately trended higher in i.p. sites for B16-F1 and B16-AAD, but trended higher in s.c. sites for B16-OVA (Fig. 6e). The low proportion of $CD4^+$ cells among B16-OVA i.p. is explained by the finding that B cells were most prevalent among B16-OVA i.p. ($44 \pm 16\%$, Fig. 6f).

Immune infiltration has been linked to intratumoral vascular abnormalities in human cancers [23]. We wished to determine whether the distributions of immune cells in Immunotypes B and C were related to differences in vascular density. One hypothesis is that the more diffuse pattern of infiltrates seen related to Immunotype C in B16-AAD i.p. tumors compared to their s.c. counterparts is related to greater vascular density, which allows immune cells to

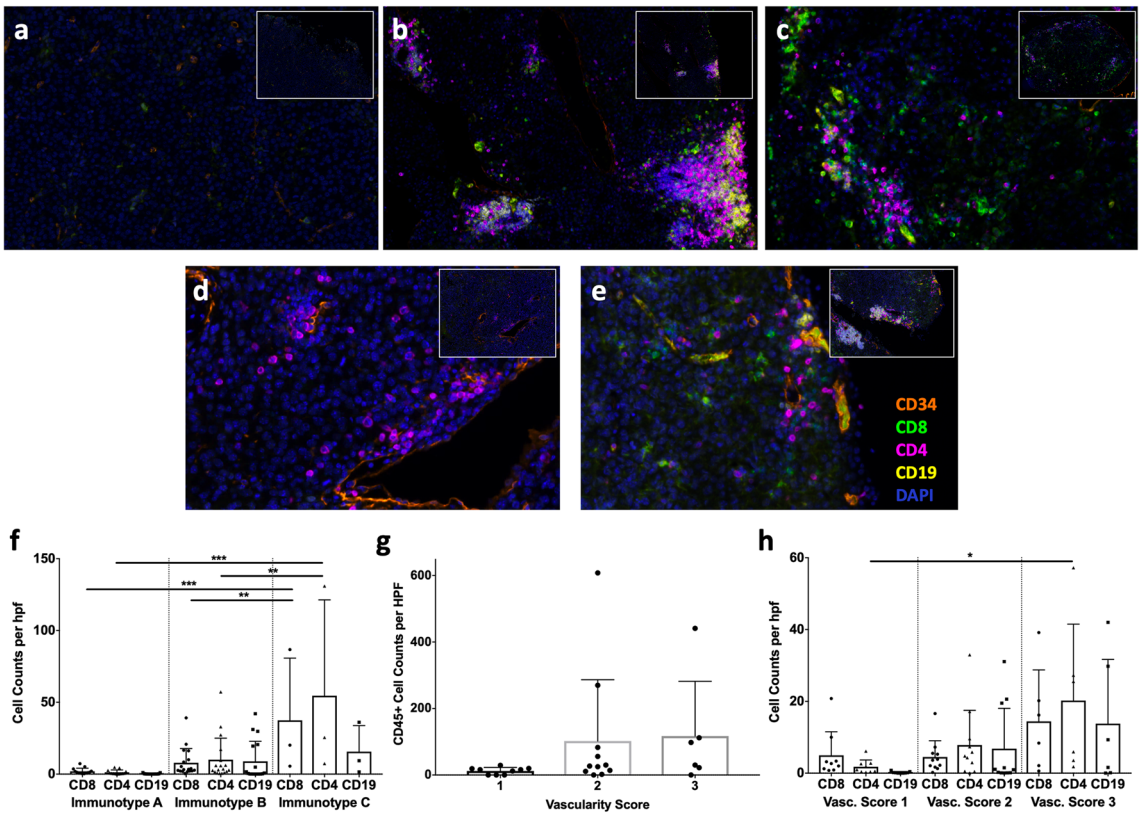

Fig. 5 Immune-cell subset characterization based on immunotype and vascularity in B16 melanomas. All tumors were stained with antibodies to CD34 (orange), CD8 (green), CD4 (magenta), CD19 (yellow), and DAPI (blue) and immune-cell subsets were enumerated. (**a**) A representative image of a s.c. B16-F1 tumor classified as Immunotype A. (**b**) An i.p. B16-OVA tumor categorized as Immunotype B with a tertiary lymphoid structure (TLS). (**c**) An i.p. B16-AAD tumor of melanoma classified as Immunotype C. (**d**) A B16-OVA s.c. tumor classified as Immunotype B with perivascular cuffing and without TLS. (**e**) A B16-AAD i.p. tumor classified as Immunotype B with perivascular cuffing independent of a TLS on high-power view, as well as a TLS in the inset. A low-power inset is provided in the right upper corner of each image. $CD8^+$ T cells, $CD4^+$ T cells, and $CD19^+$ B cells were quantified for Immunotype A, Immunotype B, and Immunotype C tumors (**f**). B16 melanomas were evaluated for associations of vascularity with $CD45^+$ cell counts (**g**), and $CD8^+$ and $CD4^+$ T-cell counts, and $CD19^+$ B-cell counts (**h**). Differences were assessed by one-way ANOVA, with significance noted by asterisks: * < 0.05, ** < 0.01, *** < 0.001, **** < 0.0001. *vasc* vascularity

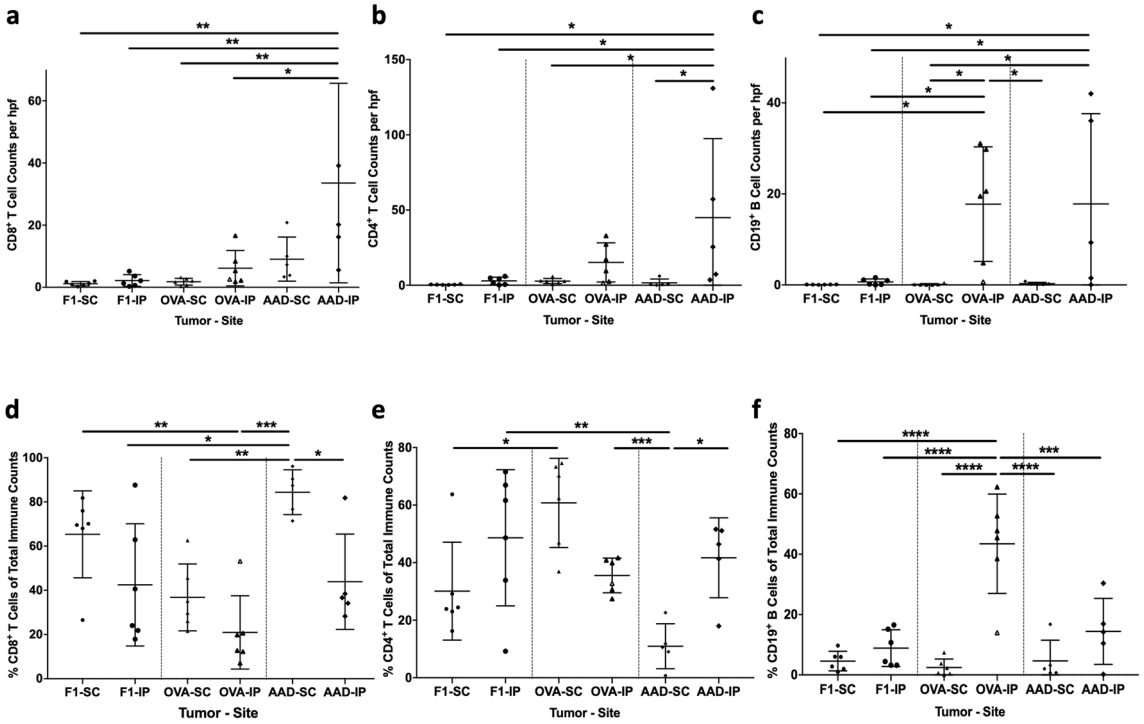

Fig. 6 Characterization of CD8 $^{+}$, CD4+, and CD19+ immune-cell subsets in B16 melanomas. B16-F1 melanomas, or those transfected with OVA or AAD, in s.c. or i.p. locations were evaluated for $CD8^+$ T-cell counts (**a**), $CD4^+$ T-cell counts (**b**), and $CD19^+$ B-cell counts (**c**). The percentage of $CD8^+$ T cells comprising the sum of CD8, CD4, and CD19 cell counts in each tumor type at both s.c. and i.p. locations (**d**), and the percentage of $CD4^+$ T cells (**e**) and $CD19^+$ B cells (**f**) of the total cell counts. Differences were assessed by one-way ANOVA, with significance noted by asterisks: * < 0.05, ** < 0.01, *** < 0.001, **** < 0.0001

infiltrate at more distributed points within the tumor mass and results in a diffuse distribution within the tumor. An alternative hypothesis is that increased vascular density provides greater opportunities for perivascular immune-cell clustering, thus leading to Immunotype B. Vascular density was significantly greater in B16-AAD i.p. tumors compared to their B16-AAD s.c. tumors, consistent with an association between increased density and Immunotype C (Fig. 4d). However, vascular density was also significantly higher in B16-F1 i.p. tumors compared to B16-F1 s.c., and trended higher for B16-OVA i.p. compared to B16-OVA s.c. tumors (Fig. 4d). Thus, differences in vascularity are inherent within s.c. versus i.p. compartments of all B16 tumor models. In addition, there were trends towards higher vascularity in association with higher $CD45^+$, $CD8^+$, $CD4^+$, and $CD19^+$ immune-cell density; however, this was only significant for $CD4^+$ T-cell infiltration (Fig. 5g, h). While the results do not rule out a possible role for increased vascular density in supporting the development of Immunotype C, any such role appears to be subservient to factors such as the overall strength of the immune response.

We also have considered whether variations in immune-cell subsets related to immunotype could be explained by the formation of tertiary lymphoid structures (TLS) in selected immunotypes. TLS contain high endothelial venule-like vasculature, which can enable naïve T cells to enter tumor tissue [24], and TLS have been associated in some studies with $CD8^+$ T-cell infiltrates [24, 25]; however, direct associations with immunotype remain to be explored. Thus, it is tempting to imagine that formation of tertiary lymphoid structures could be contributory to immunotypes. However, B-cell clusters are a key component of TLS, but B-cell densities are highest for B16-OVA i.p. Prominent B/T-cell clusters were observed in all B16-OVA i.p. tumors, examples of which are shown in Fig. 5b, e (inset). TLS were also observed in some B16-AAD i.p. tumors, but were less prominent (data not shown). This finding of TLS and B-cell dominance in B16-OVA i.p., all of which are Immunotype B, could suggest that the perivascular immune-cell-cuffing characteristic of Immunotype B can be explained simply by high prevalence of TLS in those tumors. However, a large proportion of the perivascular infiltrates in Immunotype B tumors consist mostly of $CD4^+$ and $CD8^+$ T cells, without any B-cell clusters [Fig. 5d, e (high-power image)]. In addition, as previously reported [24], TLS are not seen in s.c. sites (Fig. 5d), but only in i.p. (Fig. 5b, e). Nonetheless, Immunotype B tumors are found in both locations. Thus, these findings suggest that TLS alone do not determine

immunotype. Immunotype B histology reflects infiltrates of T cells primarily limited to perivascular locations, plus some TLS in those locations. On the other hand, among Immunotype C tumors, we found that the immune-cell composition among tumor cells (distant from vasculature) was almost completely comprised of T cells ($CD4^+$ and $CD8^+$) (Fig. 5c, and data not shown), suggesting that Immunotype C histology in B16-AAD i.p. tumors is primarily a T-cell phenomenon.

Discussion

In the present study, we identified characteristic immunotypes in murine B16 and Braf/Pten models that match immunotypes observed in human melanoma metastases [1]. In particular, we found that Immunotype A (a "cold" or non-inflamed tumor) can be modeled by B16-F1 implantable tumors or the spontaneous Braf/Pten or Braf/Pten/β-catenin tumors. On the other hand, Immunotype B (inflamed but with immune cells only cuffing intratumoral vasculature) can be modeled by B16-OVA tumors (i.p. or s.c.) or by B16-AAD tumors (s.c. only). Diffuse infiltrates (Immunotype C) were identified only in B16-AAD melanomas growing intraperitoneally. Our work identifies both antigen expression and tumor location as critical determinants of immunotype in murine models.

Findings from this study demonstrate the central role that immune responses to strong antigens play in distinguishing Immunotypes B and C from Immunotype A. Thus, we have established that Braf/Pten tumors, which are rapidly induced by activation of oncogenic driver genes with little time for accumulation of genomic mutations, are Immunotype A, while B16 tumors expressing either OVA or AAD are Immunotype B or C. Strong immunodominant peptides are generated from the OVA protein, and presented either by MHC-I or MHC-II molecules [26, 27] to $CD8^+$ and $CD4^+$ T cells, respectively. AAD is a xenogeneic cell-surface MHC molecule and thus may be recognized by the TCR as foreign MHC. One can expect that it will present thousands of peptide antigens derived from the B16 proteins, all of which could be considered neoantigens since the host is otherwise naïve to AAD-presented peptides. In addition, AAD may itself be processed intracellularly and presented to T cells, and because it is a surface protein, it may be recognized by murine B cells and antibodies. Thus, AAD may be particularly effective at inducing diffuse infiltrates related to its broad antigenicity.

On the other hand, it is surprising that B16-F1 tumors are Immunotype A: over five hundred somatic mutations have been identified in B16 melanomas, 76% of which have been predicted to be presented by murine MHC molecules [16]. In murine models using a series of melanoma cell lines with defined genetic driver mutations and a low number of somatic mutations (YUMM), immune infiltration is low [28]; however, increasing the number of somatic mutations in the YUMM tumors (YUMMER) leads to more robust immune infiltrates [29]. In addition, increased mutational load has been reported to lead to more inflamed tumors in humans [30, 31]. However, it is notable that several studies suggest that the vast majority of neoantigens are immunologically silent [32, 33], or induce responses that cross-react with normal host proteins, and thus may be subject to self-tolerance [16]. Our results suggest that a high mutational load does not necessarily translate to strong neoantigens that are sufficient to induce an inflamed tumor microenvironment, a finding that is consistent with human data from The Cancer Genome Atlas [34, 35].

The fact that high neoantigen load in B16-F1 is insufficient to induce meaningful inflammation also raises the possibility that B16-F1 tumors may have intrinsic features that limit T-cell infiltration. On one hand, low-level expression of critical homing receptor ligands on the endothelium may fail to recruit immune cells from circulation. Interestingly, expression of homing receptor ligands by intratumoral endothelium [17, 18], and of critical chemokines such as CXCL10, is enhanced by IFNγ or other cytokines [17, 36–38], suggesting a feedback loop that enhances immune infiltration and immune signatures once a certain threshold of activation occurs. This could explain why the dramatic change in antigenicity of B16-AAD can lead to Immunotype C tumors. On the other hand, different subsets of human melanomas are characterized by one or more of the following possible mechanisms of T-cell exclusion: enhanced WNT/β-catenin signaling, expression of endothelin receptor B, or overexpression of mechanical barrier molecules [39–41], which may be impenetrable by immune cells or require a specific threshold of antigen activation to be breached.

There is notable enhancement in immune-cell infiltration and/or immunotype for i.p. tumors compared to s.c. tumors generally (Fig. 4b). The fact that Immunotype C is common only in i.p, but not in s.c. sites for B16-AAD tumors suggests that some aspect of i.p. locationdrives formation of Immunotype C. Interestingly, there were substantial differences in the dominant immune-cell types in immune infiltrates as a function of tumor antigen as well as tissue site (Fig. 6). The impact of tissue site on immune infiltration and immunotype has not been well-explored and may be crucial to addressing the heterogeneity of immune response efficacy to different tumors in the same patient. Prior work has shown that the homing receptor ligands required for T-cell infiltration differ for metastases in different sites [17, 18] and that vaccines administered in different sites (s.c. vs i.v.) mediate T-cell accumulation in different visceral or soft tissues [42]. The proximity of i.p. tumors to the gut raises

interesting questions of whether the gut microbiome may contribute to the observed findings, and this deserves further investigation. Regardless, the findings of the present work further highlight the critical influence of tumor location on immune-cell infiltration and immunotype, which may have greater implications for enhancing immune therapy than has previously been appreciated. Overall, our data highlight the role of antigen in immune-cell infiltration and immunotype but point out a previously unrecognized role for tissue site that is independent of the tumor antigenicity.

The route by which immune cells infiltrate peripheral tissues involves the intratumoral vasculature, and a component of the definition of Immunotype B tumors is that the infiltrates are limited to perivascular sites. Thus, one may hypothesize that vascular density or other measures may have an impact on immunotype. Intratumoral vascular density has also been identified as a positive prognostic indicator in melanoma [43, 44]. We found higher intratumoral vascular density in i.p. tumors vs. s.c. tumors, which is worth further study to understand how vascular density may be site-dependent and how that may contribute to increased immune infiltrates in i.p. tumors, and also to study the association of $CD4^+$ T cells with increased vascular density. However, the vascularity scores were very comparable for B16-F1, B16-OVA, and B16-AAD. The association of vascular density with tumor site is strikingly consistent across the different tumor types, but does not explain overall changes in immune infiltrates or immunotypes, suggesting that functional changes in the vasculature may be more crucial than the vessel density itself, and that Immunotype C may be more dependent on these functional changes as the driving force compared to Immunotypes A or B.

In summary, the present work provides documentation of features of immune-cell infiltration into commonly used murine models, along with definition of their immunotypes. This information provides a basis for employing these models for preclinical studies of combination immunotherapies to understand how they may enhance infiltration or tumor control. Our data also highlight the fact that a large number of spontaneous neoantigens may be insufficient to drive high immune infiltrates and inflamed tumors, but that even a single strong antigen may be sufficient, and that the impact may be strongly influenced by tumor location. We find it very provocative that B-cell density and TLS formation are both identified in the B16-OVA i.p. tumors, which are all Immunotype B, rather than in B16-AAD i.p. tumors, which are mostly Immunotype C. Considering that the AAD molecule (not OVA) is a cell-surface protein, we would expect a strong antibody/B-cell response to AAD. Thus, the higher prevalence of B cells in OVA tumors than in AAD tumors is a surprising finding, and will prompt future studies on the nature of immune infiltrate as a function of antigen. As we have previously reported [24], we have found that TLS are present only in i.p. tumors, but not in s.c. tumors; thus, the impact of antigen on B-cell accumulation and TLS formation cannot be considered independent of tumor site. The findings of this work also reveal that immunotype patterns do not simply reflect TLS formation, but are likely driven by multiple factors. Many questions remain, including the impact of antigenicity and location on the type and function of infiltrating immune cells, and what mechanisms are at play in B16 melanoma and in the spontaneous Braf/Pten tumors that may actively exclude immune-cell infiltration. Furthermore, the findings raise provocative and critical questions about the roles of antigen type, breadth of immune response, tumor location, and vascularity in immune-cell infiltration patterns (immunotype) and density. We hope that these findings will lead to new work to define mechanisms explaining these findings, and to define which human tumors can be rendered responsive to immunotherapy by modulation of the same processes that have impact in these murine models.

Author contributions KML, JP, CLS Jr., VHE, and MWB conceived and designed the experiments. KML, JP, DHD, ISM, SJY, and ANW carried out the experiments and contributed to data analysis. KML, JP, CLS Jr., VHE, and MWB contributed to interpretation of the results. KML, CLS Jr., and VHE wrote the manuscript. All authors provided critical feedback and helped shape the research, analysis, and manuscript.

Funding Support was provided by United States Public Health Services Research Grants R01 CA78400 (VH Engelhard) and R01 CA057653 (CL Slingluff), United States Public Health Services Training Grants in Surgical Oncology T32 CA163177 (KM Leick), and in Immunology T32 AI007496 (J Pinczewski and AN Woods), United States Public Health Services Cancer Center Support Grant P30 CA44579 (University of Virginia Biorepository and Tissue Procurement Facility).

Compliance with ethical standards

Conflict of interest The authors declare that they have no conflicts of interest pertaining to this work.

Ethical approval and ethical standards All procedures performed in studies involving human participants/tissues were in accordance with the ethical standards of the institutional and/or national research committee and with the 1964 Helsinki declaration and its later amendments or comparable ethical standards. Use of human tissues was approved by the University of Virginia Institutional Review Board (Protocol 10598). The animal study was approved by the University of Virginia Animal Care and Use Committee (IACUC Protocol 1068). All protocols and procedures used in this study were approved by and performed in accordance with the ethical standards of the University of Virginia Animal Care and Use Committee and with the National Institute of Health's Guidelines for the Care and Use of Laboratory Animals.

Informed consent The University of Virginia Institutional Review Board protocol 10598 includes a waiver of informed consent regarding the human tissue samples used in this study.

Animal source C57BL/6 mice were purchased from NCI-Frederick Animal Production Program. All mice were maintained in pathogen-free facilities.

Cell-line authentication The C57BL/6-derived melanoma cell line B16-F1 (CRL-6323) was obtained from the American-Type Culture Collection (Manassas, VA). Transfectants expressing ovalbumin or AAD were produced as described elsewhere [19, 20]. All lines were mycoplasma negative and used within ten passages. Expression of OVA and AAD after cell passages was confirmed by flow cytometry. All lines grew readily in immunocompetent syngeneic C57BL/6 mice to form pigmented tumors typical of melanoma.

References

1. Erdag G, Schaefer JT, Smolkin ME, Deacon DH, Shea SM, Dengel LT, Patterson JW, Slingluff CL Jr (2012) Immunotype and immunohistologic characteristics of tumor-infiltrating immune cells are associated with clinical outcome in metastatic melanoma. Cancer Res 72(5):1070. https://doi.org/10.1158/0008-5472.can-11-3218
2. Bogunovic D, O'Neill DW, Belitskaya-Levy I, Vacic V, Yu YL, Adams S, Darvishian F, Berman R, Shapiro R, Pavlick AC, Lonardi S, Zavadil J, Osman I, Bhardwaj N (2009) Immune profile and mitotic index of metastatic melanoma lesions enhance clinical staging in predicting patient survival. Proc Natl Acad Sci USA 106(48):20429. https://doi.org/10.1073/pnas.0905139106
3. Mihm MC Jr, Clemente CG, Cascinelli N (1996) Tumor infiltrating lymphocytes in lymph node melanoma metastases: a histopathologic prognostic indicator and an expression of local immune response. Lab Invest 74(1):43
4. Wu X, Li J, Connolly EM, Liao X, Ouyang J, Giobbie-Hurder A, Lawrence D,McDermott D, Murphy G, Zhou J, Piesche M, Dranoff G, Rodig S, Shipp M, Hodi FS (2017) Combined anti-VEGF and anti-CTLA-4 therapy elicits humoral immunity to Galectin-1 which is associated with favorable clinical outcomes. Cancer Immunol Res 5(6):446–454. https://doi.org/10.1158/2326-6066.cir-16-0385
5. Yuan J, Adamow M, Ginsberg BA, Rasalan TS, Ritter E, Gallardo HF, Xu Y, Pogoriler E, Terzulli SL, Kuk D, Panageas KS, Ritter G, Sznol M, Halaban R, Jungbluth AA, Allison JP, Old LJ, Wolchok JD, Gnjatic S (2011) Integrated NY-ESO-1 antibody and CD8+T-cell responses correlate with clinical benefit in advanced melanoma patients treated with ipilimumab. Proc Natl Acad Sci U S A 108(40):16723–16728. https://doi.org/10.1073/pnas.1110814108
6. Hamid O, Schmidt H, Nissan A, Ridolfi L, Aamdal S, Hansson J, Guida M, Hyams DM, Gomez H, Bastholt L, Chasalow SD, Berman D (2011) A prospective phase II trial exploring the association between tumor microenvironment biomarkers and clinical activity of ipilimumab in advanced melanoma. J Trans Med 9:204. https://doi.org/10.1186/1479-5876-9-204
7. Gough M, Crittenden M, Thanarajasingam U, Sanchez-Perez L, Thompson J, Jevremovic D, Vile R (2005) Gene therapy to manipulate effector T cell trafficking to tumors for immunotherapy. J Immunol (Baltimore, Md : 1950) 174(9):5766–5773
8. Herbst RS, Soria JC, Kowanetz M, Fine GD, Hamid O, Gordon MS, Sosman JA, McDermott DF, Powderly JD, Gettinger SN, Kohrt HE, Horn L, Lawrence DP, Rost S, Leabman M, Xiao Y, Mokatrin A, Koeppen H, Hegde PS, Mellman I, Chen DS, Hodi FS (2014) Predictive correlates of response to the anti-PD-L1 antibody MPDL3280A in cancer patients. Nature 515(7528):563–567. https://doi.org/10.1038/nature14011
9. Damsky WE, Curley DP, Santhanakrishnan M, Rosenbaum LE, Platt JT, Gould Rothberg BE, Taketo MM, Dankort D, Rimm DL, McMahon M, Bosenberg M (2011) β-catenin signaling controls metastasis in Braf-activated Pten-deficient melanomas. Cancer Cell 20(6):741–754. https://doi.org/10.1016/j.ccr.2011.10.030
10. Dankort D, Curley DP, Cartlidge RA, Nelson B, Karnezis AN, Damsky WE Jr, You MJ, DePinho RA, McMahon M, Bosenberg M (2009) Braf(V600E) cooperates with Pten loss to induce metastatic melanoma. Nat Genet 41(5):544. https://doi.org/10.1038/ng.356
11. Peske JD, Thompson ED, Gemta L, Baylis RA, Fu YX, Engelhard VH (2015) Effector lymphocyte-induced lymph node-like vasculature enables naive T-cell entry into tumours and enhanced anti-tumour immunity. Nature Commun 6:7114. https://doi.org/10.1038/ncomms8114
12. Peng W, Chen JQ, Liu C, Malu S, Creasy C, Tetzlaff MT, Xu C, McKenzie JA, Zhang C, Liang X, Williams LJ, Deng W, Chen G, Mbofung R, Lazar AJ, Torres-Cabala CA, Cooper ZA, Chen PL, Tieu TN, Spranger S, Yu X, Bernatchez C, Forget MA, Haymaker C, Amaria R, McQuade JL, Glitza IC, Cascone T, Li HS, Kwong LN, Heffernan TP, Hu J, Bassett RL, Bosenberg MW, Woodman SE, Overwijk WW, Lizée G, Roszik J, Gajewski TF, Wargo JA, Gershenwald JE, Radvanyi L, Davies MA, Hwu P (2016) Loss of PTEN promotes resistance to T cell-mediated immunotherapy. Cancer Discov 6(2):202–216. https://doi.org/10.1158/2159-8290.cd-15-0283
13. Ho PC, Meeth KM, Tsui YC, Srivastava B, Bosenberg MW, Kaech SM (2014) Immune-based antitumor effects of BRAF inhibitors rely on signaling by CD40L and IFNγ. Cancer Res 74(12):3205–3217. https://doi.org/10.1158/0008-5472.can-13-3461
14. Alexandrov LB, Nik-Zainal S, Wedge DC, Aparicio SA, Behjati S, Biankin AV, Bignell GR, Bolli N, Borg A, Børresen-Dale AL, Boyault S, Burkhardt B, Butler AP, Caldas C, Davies HR, Desmedt C, Eils R, Eyfjörd JE, Foekens JA, Greaves M, Hosoda F, Hutter B, Ilicic T, Imbeaud S, Imielinsk M, Jäger N, Jones DT, Jones D, Knappskog S, Kool M, Lakhani SR, López-Otín C, Martin S, Munshi NC, Nakamura H, Northcott PA, Pajic M, Papaemmanuil E, Paradiso A, Pearson JV, Puente XS, Raine K, Ramakrishna M, Richardson AL, Richter J, Rosenstiel P, Schlesner M, Schumacher TN, Span PN, Teague JW, Totoki Y, Tutt AN, Valdés-Mas R, van`t Buuren MM, van Veer L, Vincent-Salomon A, Waddell N, Yates LR, Zucman-Rossi J, Futreal PA, McDermott U, Lichter P, Meyerson M, Grimmond SM, Siebert R, Campo E, Shibata T, Pfister SM, Campbell PJ, Stratton MR (2013) Signatures of mutational processes in human cancer. Nature 500(7463):415–421. https://doi.org/10.1038/nature12477
15. Parker SC, Gartner J, Cardenas-Navia I, Wei X, Ozel Abaan H, Ajay SS, Hansen NF, Song L, Bhanot UK, Killian JK, Gindin Y, Walker RL, Meltzer PS, Mullikin JC, Furey TS, Crawford GE, Rosenberg SA, Samuels Y, Margulies EH (2012) Mutational signatures of de-differentiation in functional non-coding regions of melanoma genomes. PLoS Genet 8(8):e1002871. https://doi.org/10.1371/journal.pgen.1002871
16. Castle JC, Kreiter S, Diekmann J, Lower M, van de Roemer N, de GJ, Selmi A, Diken M, Boegel S, Paret C, Koslowski M, Kuhn AN, Britten CM, Huber C, Tureci O, Sahin U (2012) Exploiting the mutanome for tumor vaccination. Cancer Res 72(5):1081–1091
17. Woods AN, Wilson AL, Srivinisan N, Zeng J, Dutta AB, Peske JD, Tewalt EF, Gregg RK, Ferguson AR, Engelhard VH (2017) Differential expression of homing receptor ligands on tumor-associated vasculature that control CD8 effector T-cell entry. Cancer Immunol Res 5(12):1062–1073. https://doi.org/10.1158/2326-6066.cir-17-0190
18. Peske JD, Woods AB, Engelhard VH (2015) Control of CD8 T-cell infiltration into tumors by vasculature and microenvironment.

Adv Cancer Res 128:263–307. https://doi.org/10.1016/bs.acr.2015.05.001
19. Hargadon KM, Brinkman CC, Sheasley-O'neill SL, Nichols LA, Bullock TN, Engelhard VH (2006) Incomplete differentiation of antigen-specific CD8 T cells in tumor-draining lymph nodes. JImmunol 177(9):6081
20. Mullins DW, Bullock TN, Colella TA, Robila VV, Engelhard VH (2001) Immune responses to the HLA-A*0201-restricted epitopes of tyrosinase and glycoprotein 100 enable control of melanoma outgrowth in HLA-A*0201-transgenic mice. J Immunol 167(9):4853
21. Newberg MH, Smith DH, Haertel SB, Vining DR, Lacy E, Engelhard VH (1996) Importance of MHC class 1 alpha2 and alpha3 domains in the recognition of self and non-self MHC molecules. J Immunol 156(7):2473
22. Spranger S, Bao R, Gajewski TF (2015) Melanoma-intrinsic beta-catenin signalling prevents anti-tumour immunity. Nature 523(7559):231. https://doi.org/10.1038/nature14404
23. Neilson D, MacPherson S, Townsend KN, Lum JJ (2014) Tumor vascularity in ovarian cancer: T cells need breathing room. Oncoimmunology 3:e28272. https://doi.org/10.4161/onci.28272
24. Engelhard VH, Rodriguez AB, Mauldin IS, Woods AN, Peske JD, Slingluff CL Jr (2018) Immune cell infiltration and tertiary lymphoid structures as determinants of antitumor immunity. J Immunol (Baltimore; Md : 1950) 200(2):432–442. https://doi.org/10.4049/jimmunol.1701269
25. Hiraoka N, Ino Y, Yamazaki-Itoh R (2016) Tertiary lymphoid organs in cancer tissues. Front Immunol 7:244. https://doi.org/10.3389/fimmu.2016.00244
26. Rotzschke O, Falk K, Stevanovic S, Jung G, Walden P, Rammensee HG (1991) Exact prediction of a natural T cell epitope. Eur J Immunol 21(11):2891–2894. https://doi.org/10.1002/eji.1830211136
27. Robertson JM, Jensen PE, Evavold BD (2000) DO11.10 and OT-II T cells recognize a C-terminal ovalbumin 323-339 epitope. J Immunol 164(9):4706–4712
28. Meeth K, Wang JX, Micevic G, Damsky W, Bosenberg MW (2016) The YUMM lines: a series of congenic mouse melanoma cell lines with defined genetic alterations. Pigment Cell Melanoma Res 29(5):590–597. https://doi.org/10.1111/pcmr.12498
29. Wang J, Perry CJ, Meeth K, Thakral D, Damsky W, Micevic G, Kaech S, Blenman K, Bosenberg M (2017) UV-induced somatic mutations elicit a functional T cell response in the YUMMER mouse melanoma model. Pigment Cell Melanoma Res 30(4):428–435. https://doi.org/10.1111/pcmr.12591
30. Brown SD, Warren RL, Gibb EA, Martin SD, Spinelli JJ, Nelson BH, Holt RA (2014) Neo-antigens predicted by tumor genome meta-analysis correlate with increased patient survival. Genome Res 24(5):743–750. https://doi.org/10.1101/gr.165985.113
31. Efremova M, Finotello F, Rieder D, Trajanoski Z (2017) Neoantigens generated by individual mutations and their role in cancer immunity and immunotherapy. Front Immunol 8:1679. https://doi.org/10.3389/fimmu.2017.01679
32. Carreno BM, Magrini V, Becker-Hapak M, Kaabinejadian S, Hundal J, Petti AA, Ly A, Lie WR, Hildebrand WH, Mardis ER, Linette GP (2015) Cancer immunotherapy a dendritic cell vaccine increases the breadth and diversity of melanoma neoantigen-specific T cells. Science 348(6236):803–808. https://doi.org/10.1126/science.aaa3828
33. Yadav M, Jhunjhunwala S, Phung QT, Lupardus P, Tanguay J, Bumbaca S, Franci C, Cheung TK, Fritsche J, Weinschenk T, Modrusan Z, Mellman I, Lill JR, Delamarre L (2014) Predicting immunogenic tumour mutations by combining mass spectrometry and exome sequencing. Nature 515(7528):572–576. https://doi.org/10.1038/nature14001
34. Spranger S, Luke JJ, Bao R, Zha Y, Hernandez KM, Li Y, Gajewski AP, Andrade J, Gajewski TF (2016) Density of immunogenic antigens does not explain the presence or absence of the T-cell-inflamed tumor microenvironment in melanoma. Proc Natl Acad Sci U S A 113(48):E7759–e7768. https://doi.org/10.1073/pnas.1609376113
35. Danilova L, Wang H, Sunshine J, Kaunitz GJ, Cottrell TR, Xu H, Esandrio J, Anders RA, Cope L, Pardoll DM, Drake CG, Taube JM (2016) Association of PD-1/PD-L axis expression with cytolytic activity, mutational load, and prognosis in melanoma and other solid tumors. Proc Natl Acad Sci USA 113(48):E7769–e7777. https://doi.org/10.1073/pnas.1607836113
36. Clancy-Thompson E, Perekslis TJ, Croteau W, Alexander MP, Chabanet TB, Turk MJ, Huang YH, Mullins DW (2015) Melanoma induces, and adenosine suppresses, CXCR2-cognate chemokine production and t-cell infiltration of lungs bearing metastatic-like disease. Cancer Immunol Res 3(8):956–967. https://doi.org/10.1158/2326-6066.cir-15-0015
37. Mauldin IS, Wages NA, Stowman AM, Wang E, Smolkin ME, Olson WC, Deacon DH, Smith KT, Galeassi NV, Chianese-Bullock KA, Dengel LT, Marincola FM, Petroni GR, Mullins DW, Slingluff CL Jr (2016) Intratumoral interferon-gamma increases chemokine production but fails to increase T cell infiltration of human melanoma metastases. Cancer Immunol Immunother. https://doi.org/10.1007/s00262-016-1881-y
38. Hailemichael Y, Woods A, Fu T, He Q, Nielsen MC, Hasan F, Roszik J, Xiao Z, Vianden C, Khong H, Singh M, Sharma M, Faak F, Moore D, Dai Z, Anthony SM, Schluns KS, Sharma P, Engelhard VH, Overwijk WW (2018) Cancer vaccine formulation dictates synergy with CTLA-4 and PD-L1 checkpoint blockade therapy. J Clin Invest. https://doi.org/10.1172/jci93303
39. Spranger S, Gajewski TF (2015) A new paradigm for tumor immune escape: beta-catenin-driven immune exclusion. J Immunother Cancer 3:43. https://doi.org/10.1186/s40425-015-0089-6
40. Buckanovich RJ, Facciabene A, Kim S, Benencia F, Sasaroli D, Balint K, Katsaros D, O'Brien-Jenkins A, Gimotty PA, Coukos G (2008) Endothelin B receptor mediates the endothelial barrier to T cell homing to tumors and disables immune therapy. Nat Med 14(1):28–36
41. Salerno EP, Bedognetti D, Mauldin IS, Deacon DH, Shea SM, Pinczewski J, Obeid JM, Coukos G, Wang E, Gajewski TF, Marincola FM, Slingluff CL (2016) Human melanomas and ovarian cancers overexpressing mechanical barrier molecule genes lack immune signatures and have increased patient mortality risk. Oncoimmunology 5(12):e1240857. https://doi.org/10.1080/2162402x.2016.1240857
42. Mullins DW, Sheasley SL, Ream RM, Bullock TN, FuYX, Engelhard VH (2003) Route of immunization with peptide-pulsed dendritic cells controls the distribution of memory and effector T cells in lymphoid tissues and determines the pattern of regional tumor control. J Exp Med 198(7):1023–1034
43. Martinet L, Le Guellec S, Filleron T, Lamant L, Meyer N, Rochaix P, Garrido I, Girard JP (2012) High endothelial venules (HEVs) in human melanoma lesions: major gateways for tumor-infiltrating lymphocytes. Oncoimmunology 1(6):829–839. https://doi.org/10.4161/onci.20492
44. Messina JL, Fenstermacher DA, Eschrich S, Qu X, Berglund AE, Lloyd MC, Schell MJ, Sondak VK, Weber JS, Mule JJ (2012) 12-Chemokine gene signature identifies lymph node-like structures in melanoma: potential for patient selection for immunotherapy? Sci Rep 2:765. https://doi.org/10.1038/srep00765